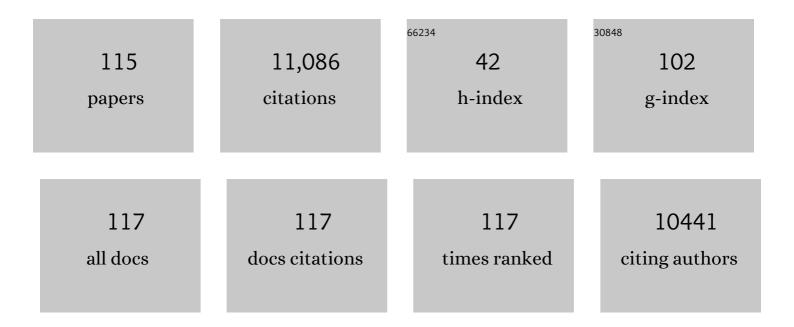
List of Publications by Year in descending order

Source: https://exaly.com/author-pdf/2070742/publications.pdf Version: 2024-02-01



#	Article	IF	CITATIONS
1	Single platinum atoms immobilized on an MXene as an efficient catalyst for the hydrogen evolution reaction. Nature Catalysis, 2018, 1, 985-992.	16.1	1,236
2	Filling the oxygen vacancies in Co <sub>3</sub> O <sub>4</sub> with phosphorus: an ultra-efficient electrocatalyst for overall water splitting. Energy and Environmental Science, 2017, 10, 2563-2569.	15.6	859
3	Boron-doped nitrogen-deficient carbon nitride-based Z-scheme heterostructures for photocatalytic overall water splitting. Nature Energy, 2021, 6, 388-397.	19.8	764
4	<i>Operando</i> Identification of the Dynamic Behavior of Oxygen Vacancy-Rich Co <sub>3</sub> O <sub>4</sub> for Oxygen Evolution Reaction. Journal of the American Chemical Society, 2020, 142, 12087-12095.	6.6	736
5	Tuning the Coordination Environment in Single-Atom Catalysts to Achieve Highly Efficient Oxygen Reduction Reactions. Journal of the American Chemical Society, 2019, 141, 20118-20126.	6.6	683
6	Synergy of Dopants and Defects in Graphitic Carbon Nitride with Exceptionally Modulated Band Structures for Efficient Photocatalytic Oxygen Evolution. Advanced Materials, 2019, 31, e1903545.	11.1	604
7	Controlling the Oxidation State of the Cu Electrode and Reaction Intermediates for Electrochemical CO <sub>2</sub> Reduction to Ethylene. Journal of the American Chemical Society, 2020, 142, 2857-2867.	6.6	342
8	Preferential Cation Vacancies in Perovskite Hydroxide for the Oxygen Evolution Reaction. Angewandte Chemie - International Edition, 2018, 57, 8691-8696.	7.2	337
9	Atomic cale CoO <i><sub>x</sub></i> Species in Metal–Organic Frameworks for Oxygen Evolution Reaction. Advanced Functional Materials, 2017, 27, 1702546.	7.8	327
10	Zirconiumâ€Regulationâ€Induced Bifunctionality in 3D Cobalt–Iron Oxide Nanosheets for Overall Water Splitting. Advanced Materials, 2019, 31, e1901439.	11.1	306
11	Tuning the Selective Adsorption Site of Biomass on Co <sub>3</sub> O <sub>4</sub> by Ir Single Atoms for Electrosynthesis. Advanced Materials, 2021, 33, e2007056.	11.1	217
12	Identifying the Geometric Site Dependence of Spinel Oxides for the Electrooxidation of 5â€Hydroxymethylfurfural. Angewandte Chemie - International Edition, 2020, 59, 19215-19221.	7.2	211
13	Unveiling the Electrooxidation of Urea: Intramolecular Coupling of the Nâ^'N Bond. Angewandte Chemie - International Edition, 2021, 60, 7297-7307.	7.2	204
14	Molecular Design of Polymer Heterojunctions for Efficient Solar–Hydrogen Conversion. Advanced Materials, 2017, 29, 1606198.	11.1	203
15	Defectâ€Induced Pt–Co–Se Coordinated Sites with Highly Asymmetrical Electronic Distribution for Boosting Oxygenâ€Involving Electrocatalysis. Advanced Materials, 2019, 31, e1805581.	11.1	168
16	A [001]â€Oriented Hittorf's Phosphorus Nanorods/Polymeric Carbon Nitride Heterostructure for Boosting Wideâ€Spectrumâ€Responsive Photocatalytic Hydrogen Evolution from Pure Water. Angewandte Chemie - International Edition, 2020, 59, 868-873.	7.2	164
17	Tailoring Competitive Adsorption Sites by Oxygenâ€Vacancy on Cobalt Oxides to Enhance the Electrooxidation of Biomass. Advanced Materials, 2022, 34, e2107185.	11.1	162
18	Synergy between cobalt and nickel on NiCo2O4 nanosheets promotes peroxymonosulfate activation for efficient norfloxacin degradation. Applied Catalysis B: Environmental, 2022, 306, 121091.	10.8	148

#	Article	IF	CITATIONS
19	Proton Capture Strategy for Enhancing Electrochemical CO <sub>2</sub> Reduction on Atomically Dispersed Metal–Nitrogen Active Sites**. Angewandte Chemie - International Edition, 2021, 60, 11959-11965.	7.2	144
20	Screening highly active perovskites for hydrogen-evolving reaction via unifying ionic electronegativity descriptor. Nature Communications, 2019, 10, 3755.	5.8	139
21	Utilizing ion leaching effects for achieving high oxygen-evolving performance on hybrid nanocomposite with self-optimized behaviors. Nature Communications, 2020, 11, 3376.	5.8	122
22	The Role of the Copper Oxidation State in the Electrocatalytic Reduction of CO <sub>2</sub> into Valuable Hydrocarbons. ACS Sustainable Chemistry and Engineering, 2019, 7, 1485-1492.	3.2	121
23	Voltage- and time-dependent valence state transition in cobalt oxide catalysts during the oxygen evolution reaction. Nature Communications, 2020, 11, 1984.	5.8	120
24	Operando Spectral and Electrochemical Investigation into the Heterophase Stimulated Active Species Transformation in Transition-Metal Sulfides for Efficient Electrocatalytic Oxygen Evolution. ACS Catalysis, 2020, 10, 1855-1864.	5.5	113
25	Morphology Manipulation of Copper Nanocrystals and Product Selectivity in the Electrocatalytic Reduction of Carbon Dioxide. ACS Catalysis, 2019, 9, 5217-5222.	5.5	105
26	Scalable Molten Salt Synthesis of Platinum Alloys Planted in Metal–Nitrogen–Graphene for Efficient Oxygen Reduction. Angewandte Chemie - International Edition, 2022, 61, .	7.2	102
27	Elucidation of the Synergistic Effect of Dopants and Vacancies on Promoted Selectivity for CO <sub>2</sub> Electroreduction to Formate. Advanced Materials, 2021, 33, e2005113.	11.1	95
28	Hierarchically nanostructured NiO-Co3O4 with rich interface defects for the electro-oxidation of 5-hydroxymethylfurfural. Science China Chemistry, 2020, 63, 980-986.	4.2	85
29	Probing the active site in single-atom oxygen reduction catalysts via operando X-ray and electrochemical spectroscopy. Nature Communications, 2020, 11, 4233.	5.8	80
30	Heterojunction of Zinc Blende/Wurtzite in Zn <sub>1–<i>x</i></sub> Cd <sub><i>x</i></sub> S Solid Solution for Efficient Solar Hydrogen Generation: X-ray Absorption/Diffraction Approaches. ACS Applied Materials & Interfaces, 2015, 7, 22558-22569.	4.0	74
31	Modulating the electronic structure of ultrathin layered double hydroxide nanosheets with fluorine: an efficient electrocatalyst for the oxygen evolution reaction. Journal of Materials Chemistry A, 2019, 7, 14483-14488.	5.2	73
32	Engineering the coordination geometry of metal–organic complex electrocatalysts for highly enhanced oxygen evolution reaction. Journal of Materials Chemistry A, 2018, 6, 805-810.	5.2	69
33	Electronic Structure Evolution in Tricomponent Metal Phosphides with Reduced Activation Energy for Efficient Electrocatalytic Oxygen Evolution. Small, 2018, 14, e1801756.	5.2	69
34	Defectsâ€Induced Inâ€Plane Heterophase in Cobalt Oxide Nanosheets for Oxygen Evolution Reaction. Small, 2019, 15, e1904903.	5.2	69
35	An integrated cobalt disulfide (CoS <sub>2</sub> ) co-catalyst passivation layer on silicon microwires for photoelectrochemical hydrogen evolution. Journal of Materials Chemistry A, 2015, 3, 23466-23476.	5.2	68
36	Ordered mesostructured Cu-doped TiO2 spheres as active visible-light-driven photocatalysts for degradation of paracetamol. Chemical Engineering Journal, 2014, 237, 131-137.	6.6	62

#	Article	IF	CITATIONS
37	Nanogap Engineered Plasmonâ€Enhancement in Photocatalytic Solar Hydrogen Conversion. Advanced Materials Interfaces, 2015, 2, 1500280.	1.9	55
38	Evolution of Visible Photocatalytic Properties of Cu-Doped CeO <sub>2</sub> Nanoparticles: Role of Cu <sup>2+</sup> -Mediated Oxygen Vacancies and the Mixed-Valence States of Ce Ions. ACS Sustainable Chemistry and Engineering, 2018, 6, 8536-8546.	3.2	55
39	Recent advances in vanadium pentoxide (V <sub>2</sub> O <sub>5</sub> ) towards related applications in chromogenics and beyond: fundamentals, progress, and perspectives. Journal of Materials Chemistry C, 2022, 10, 4019-4071.	2.7	53
40	Nbâ€Doped Hematite Nanorods for Efficient Solar Water Splitting: Electronic Structure Evolution versus Morphology Alteration. ChemNanoMat, 2016, 2, 704-711.	1.5	51
41	Controllable synthesis of Fe–N <sub>4</sub> species for acidic oxygen reduction. , 2020, 2, 452-460.		50
42	Mesoporous Fe-doped TiO2 sub-microspheres with enhanced photocatalytic activity under visible light illumination. Applied Catalysis B: Environmental, 2012, 127, 175-181.	10.8	48
43	5f Covalency Synergistically Boosting Oxygen Evolution of UCoO <sub>4</sub> Catalyst. Journal of the American Chemical Society, 2022, 144, 416-423.	6.6	48
44	Activated Ni–OH Bonds in a Catalyst Facilitates the Nucleophile Oxidation Reaction. Advanced Materials, 2022, 34, e2105320.	11.1	47
45	Dopingâ€Modulated Strain Enhancing the Phosphate Tolerance on PtFe Alloys for Highâ€Temperature Proton Exchange Membrane Fuel Cells. Advanced Functional Materials, 2022, 32, .	7.8	45
46	In Situ/Operando Xâ€ <b>f</b> ay Spectroscopies for Advanced Investigation of Energy Materials. Chemistry - A European Journal, 2018, 24, 18356-18373.	1.7	43
47	Tailoring lattice strain in ultra-fine high-entropy alloys for active and stable methanol oxidation. Science China Materials, 2021, 64, 2454-2466.	3.5	43
48	Atomically Dispersed Janus Nickel Sites on Red Phosphorus for Photocatalytic Overall Water Splitting. Angewandte Chemie - International Edition, 2022, 61, .	7.2	43
49	Electronic properties of free-standing TiO <sub>2</sub> nanotube arrays fabricated by electrochemical anodization. Physical Chemistry Chemical Physics, 2015, 17, 22064-22071.	1.3	42
50	Identifying the Geometric Site Dependence of Spinel Oxides for the Electrooxidation of 5â€Hydroxymethylfurfural. Angewandte Chemie, 2020, 132, 19377-19383.	1.6	41
51	A [001]â€Oriented Hittorf's Phosphorus Nanorods/Polymeric Carbon Nitride Heterostructure for Boosting Wideâ€Spectrumâ€Responsive Photocatalytic Hydrogen Evolution from Pure Water. Angewandte Chemie, 2020, 132, 878-883.	1.6	40
52	Singleâ€Metal Atoms and Ultraâ€Small Clusters Manipulating Charge Carrier Migration in Polymeric Perylene Diimide for Efficient Photocatalytic Oxygen Production. Advanced Energy Materials, 2022, 12,	10.2	40
53	Synergistic-Effect-Controlled CoTe <sub>2</sub> /Carbon Nanotube Hybrid Material for Efficient Water Oxidation. Journal of Physical Chemistry C, 2016, 120, 28093-28099.	1.5	39
54	Mechanism of Electrochemical Deposition and Coloration of Electrochromic V2O5 Nano Thin Films: an In Situ X-Ray Spectroscopy Study. Nanoscale Research Letters, 2015, 10, 387.	3.1	38

#	Article	IF	CITATIONS
55	Fe <sup>2+</sup> â€Induced In Situ Intercalation and Cation Exsolution of Co <sub>80</sub> Fe <sub>20</sub> (OH)(OCH <sub>3</sub> ) with Rich Vacancies for Boosting Oxygen Evolution Reaction. Advanced Functional Materials, 2021, 31, 2009245.	7.8	38
56	Preferential Cation Vacancies in Perovskite Hydroxide for the Oxygen Evolution Reaction. Angewandte Chemie, 2018, 130, 8827-8832.	1.6	37
57	Critical Factors Controlling Superoxide Reactions in Lithium–Oxygen Batteries. ACS Energy Letters, 2020, 5, 1355-1363.	8.8	37
58	Boronâ€Tethering and Regulative Electronic States Around Iridium Species for Hydrogen Evolution. Advanced Functional Materials, 2022, 32, .	7.8	35
59	Electrochemically Activated Reduced Graphene Oxide Used as Solid-State Symmetric Supercapacitor: An X-ray Absorption Spectroscopic Investigation. Journal of Physical Chemistry C, 2016, 120, 22134-22141.	1.5	33
60	Activating KlÃ <b>¤</b> i-Type Organometallic Precursors at Metal Oxide Surfaces for Enhanced Solar Water Oxidation. ACS Energy Letters, 2018, 3, 1613-1619.	8.8	33
61	Probing the Active Sites of Carbonâ€Encapsulated Cobalt Nanoparticles for Oxygen Reduction. Small Methods, 2019, 3, 1800439.	4.6	33
62	Tuning the Electrical and Thermoelectric Properties of N Ion Implanted SrTiO3 Thin Films and Their Conduction Mechanisms. Scientific Reports, 2019, 9, 14486.	1.6	30
63	Surface Electronic Structure Reconfiguration of Hematite Nanorods for Efficient Photoanodic Water Oxidation. Solar Rrl, 2020, 4, 1900349.	3.1	30
64	In Situ/Operando Capturing Unusual Ir <sup>6+</sup> Facilitating Ultrafast Electrocatalytic Water Oxidation. Advanced Functional Materials, 2021, 31, 2104746.	7.8	29
65	The Electro-Deposition/Dissolution of CuSO <sub>4</sub> Aqueous Electrolyte Investigated by <i>In Situ</i> Soft X-ray Absorption Spectroscopy. Journal of Physical Chemistry B, 2018, 122, 780-787.	1.2	26
66	Plasmon-Induced Visible-Light Photocatalytic Activity of Au Nanoparticle-Decorated Hollow Mesoporous TiO <sub>2</sub> : A View by X-ray Spectroscopy. Journal of Physical Chemistry C, 2018, 122, 6955-6962.	1.5	25
67	Proton Capture Strategy for Enhancing Electrochemical CO <sub>2</sub> Reduction on Atomically Dispersed Metal–Nitrogen Active Sites**. Angewandte Chemie, 2021, 133, 12066-12072.	1.6	25
68	Concave Pt–Zn Nanocubes with Highâ€Index Faceted Pt Skin as Highly Efficient Oxygen Reduction Catalyst. Advanced Science, 2022, 9, e2200147.	5.6	25
69	Plasmonâ€Enhanced Electrocatalytic Properties of Rationally Designed Hybrid Nanostructures at a Catalytic Interface. Advanced Materials Interfaces, 2019, 6, 1801144.	1.9	24
70	Unveiling the Electrooxidation of Urea: Intramolecular Coupling of the Nâ^'N Bond. Angewandte Chemie, 2021, 133, 7373-7383.	1.6	24
71	An integrated bioelectrochemical system coupled CO2 electroreduction device based on atomically dispersed iron electrocatalysts. Nano Energy, 2021, 87, 106187.	8.2	23
72	Structurally ordered highâ€entropy intermetallic nanoparticles with enhanced C–C bond cleavage for ethanol oxidation. SmartMat, 2023, 4, .	6.4	23

#	Article	IF	CITATIONS
73	Scalable Molten Salt Synthesis of Platinum Alloys Planted in Metal–Nitrogen–Graphene for Efficient Oxygen Reduction. Angewandte Chemie, 2022, 134, .	1.6	22
74	Electronically Coupled Uranium and Iron Oxide Heterojunctions as Efficient Water Oxidation Catalysts. Advanced Functional Materials, 2019, 29, 1905005.	7.8	18
75	Electronic and atomic structure of TiO2 anatase spines on sea-urchin-like microspheres by X-ray absorption spectroscopy. Applied Surface Science, 2020, 502, 144297.	3.1	18
76	Catalytically Active Site Identification of Molybdenum Disulfide as Gas Cathode in a Nonaqueous Li–CO <sub>2</sub> Battery. ACS Applied Materials & Interfaces, 2021, 13, 6156-6167.	4.0	18
77	X-ray Absorption Spectroscopic Study on Interfacial Electronic Properties of FeOOH/Reduced Graphene Oxide for Asymmetric Supercapacitors. ACS Sustainable Chemistry and Engineering, 2017, 5, 3186-3194.	3.2	17
78	Effect of Fe ion implantation on the thermoelectric properties and electronic structures of CoSb <sub>3</sub> thin films. RSC Advances, 2019, 9, 36113-36122.	1.7	17
79	Quinary Defect-Rich Ultrathin Bimetal Hydroxide Nanosheets for Water Oxidation. ACS Applied Materials & Interfaces, 2019, 11, 44018-44025.	4.0	15
80	Interlayer ligand engineering of β-Ni(OH)2 for oxygen evolution reaction. Science China Chemistry, 2020, 63, 1684-1693.	4.2	15
81	Regulating Crystal Structure and Atomic Arrangement in Single-Component Metal Oxides through Electrochemical Conversion for Efficient Overall Water Splitting. ACS Applied Materials & Interfaces, 2020, 12, 57038-57046.	4.0	15
82	In Situ Observation of the Insulator-To-Metal Transition and Nonequilibrium Phase Transition for Li <sub>1–<i>x</i></sub> CoO <sub>2</sub> Films with Preferred (003) Orientation Nanorods. ACS Applied Materials & Interfaces, 2019, 11, 33043-33053.	4.0	14
83	ldentifying the crystal and electronic structure evolution in triâ€component transition metal oxide nanosheets for efficient electrocatalytic oxygen evolution. EcoMat, 2019, 1, e12005.	6.8	14
84	Manipulating metal-oxygen local atomic structures in single-junctional p-Si/WO3 photocathodes for efficient solar hydrogen generation. Nano Research, 2021, 14, 2285.	5.8	14
85	<i>A</i> '– <i>B</i> Intersite Cooperation-Enhanced Water Splitting in Quadruple Perovskite Oxide CaCu <sub>3</sub> Ir <sub>4</sub> O <sub>12</sub> . Chemistry of Materials, 2021, 33, 9295-9305.	3.2	11
86	Rapid adsorption of industrial pollutants using metal ion doped hydroxyapatite. AIP Conference Proceedings, 2019, , .	0.3	10
87	In Situ Exfoliation and Pt Deposition of Antimonene for Formic Acid Oxidation via a Predominant Dehydrogenation Pathway. Research, 2020, 2020, 5487237.	2.8	10
88	Preparation of N- <mml:math <br="" xmlns:mml="http://www.w3.org/1998/Math/MathML">id="M1"&gt;<mml:mrow><mml:msub><mml:mrow><mml:mtext>TiO</mml:mtext></mml:mrow><mml:mtext>2 a Microwave/Sol-Gel Method and Its Photocatalytic Activity for Bisphenol A under Visible-Light and Sunlight Irradiation. International Journal of Photoenergy, 2013, 2013, 1-9.</mml:mtext></mml:msub></mml:mrow></mml:math>	<td>t&gt;</td>	t>
89	Uranium Oxide Nanocrystals by Microwaveâ€Assisted Thermal Decomposition: Electronic and Structural Properties. Zeitschrift Fur Anorganische Und Allgemeine Chemie, 2018, 644, 12-18.	0.6	8
90	Structure and Transport Properties of Nickel-Implanted CoSb <sub>3</sub> Skutterudite Thin Films	2.5	8

90 Synthesized via Pulsed Laser Deposition. ACS Applied Energy Materials, 2018, 1, 5879-5886.

#	Article	IF	CITATIONS
91	Structural evolution and Au nanoparticles enhanced photocatalytic activity of sea-urchin-like TiO2 microspheres: An X-ray absorption spectroscopy study. Applied Surface Science, 2021, 562, 150127.	3.1	8
92	Selective adsorption of greenhouse gases on the residual carbon in lignite coal liquefaction. Journal of the Taiwan Institute of Chemical Engineers, 2018, 85, 170-175.	2.7	7
93	Adsorption isotherms and kinetics of activated carbons produced from coals of different ranks. Water Science and Technology, 2015, 71, 1189-1195.	1.2	6
94	Influence of halide ions on the structure and properties of copper indium sulphide quantum dots. Chemical Communications, 2020, 56, 3341-3344.	2.2	6
95	Significant role of substrate temperature on the morphology, electronic structure and thermoelectric properties of SrTiO3 films deposited by pulsed laser deposition. Surface and Coatings Technology, 2021, 407, 126740.	2.2	6
96	Investigation of adsorption of methylene blue from aqueous phase onto coal-based activated carbons. Journal of the Chinese Institute of Engineers, Transactions of the Chinese Institute of Engineers,Series A/Chung-kuo Kung Ch'eng Hsuch K'an, 2017, 40, 355-360.	0.6	5
97	Enhancing Solarâ€Driven Water Splitting with Surfaceâ€Engineered Nanostructures. Solar Rrl, 2018, 3, 1800285.	3.1	5
98	Photo generated charge transport studies of defects-induced shuttlecock-shaped ZnO/Ag hybrid nanostructures. Nanotechnology, 2021, 32, 305708.	1.3	5
99	Au-BINOL Hybrid Nanocatalysts: Insights into the Structure-Based Enhancement of Catalytic and Photocatalytic Performance. Industrial & Engineering Chemistry Research, 2019, 58, 5479-5489.	1.8	4
100	Excitation induced enhancement of spectral response and energy transfer mechanisms in Fe/Sm modified ZnO phosphors. Journal of Applied Physics, 2020, 128, 143104.	1.1	4
101	AuPd Nanoicosahedra: Atomic-Level Surface Modulation for Optimization of Electrocatalytic and Photocatalytic Energy Conversion. ACS Applied Energy Materials, 2021, 4, 2652-2662.	2.5	4
102	Sequential tunability of red and white light emissions in Sm-activated ZnO phosphors by up- and downconversion mechanisms. Journal of Applied Physics, 2021, 129, .	1.1	4
103	Extended Graphite Supported Flower-like MnO2 as Bifunctional Materials for Supercapacitors and Glucose Sensing. Nanomaterials, 2021, 11, 2881.	1.9	4
104	A Facile Approach for Pt Single Atoms Deposition on Two-Dimensional Calcium Niobate Nanosheets for Photocatalytic Hydrogen Evolution. ACS Sustainable Chemistry and Engineering, 2022, 10, 9096-9104.	3.2	4
105	Defects assisted structural and electrical properties of Ar ion irradiated TiO2/SrTiO3 bilayer. Materials Letters, 2021, 282, 128880.	1.3	3
106	Controlled Magnetic Isolation and Decoupling of Perpendicular FePt Films by Capping Ultrathin Cu(002) Nano-Islands. Journal of Composites Science, 2021, 5, 140.	1.4	3
107	Formation of FePt–MgO Nanocomposite Films at Reduced Temperature. Journal of Composites Science, 2022, 6, 158.	1.4	3
108	Role of Interfacial Defects in Photoelectrochemical Properties of BiVO4 Coated on ZnO Nanodendrites: X-ray Spectroscopic and Microscopic Investigation. ACS Applied Materials & Interfaces, 2021, 13, 41524-41536.	4.0	2

#	Article	IF	CITATIONS
109	Multicycle Performance of CaTiO3 Decorated CaO-Based CO2 Adsorbent Prepared by a Versatile Aerosol Assisted Self-Assembly Method. Nanomaterials, 2021, 11, 3188.	1.9	2
110	Atomically Dispersed Janus Nickel Sites on Red Phosphorus for Photocatalytic Overall Water Splitting. Angewandte Chemie, 0, , .	1.6	2
111	Formation of a pâ€n heterojunction photocatalyst by the interfacing of graphitic carbon nitride and delafossite <scp>CuGaO<sub>2</sub></scp> . Journal of the Chinese Chemical Society, 2022, 69, 1042-1050.	0.8	2
112	Probing reversal of orbital symmetry in CaCu3-xTi4-xFe2xO12 (x = 0.0–0.7) by X-ray absorption spectroscopy. Journal of Materials Science: Materials in Electronics, 2021, 32, 13630-13638.	1.1	1
113	Understanding the role of structural distortions on the transport properties of Ar ion irradiated SrTiO3 thin films: X-ray absorption investigation. Journal of Applied Physics, 2021, 130, .	1.1	1
114	Plasmonic Nanoparticles: Plasmon-Enhanced Electrocatalytic Properties of Rationally Designed Hybrid Nanostructures at a Catalytic Interface (Adv. Mater. Interfaces 2/2019). Advanced Materials Interfaces, 2019, 6, 1970011.	1.9	0
115	(Invited) In Situ/Operando Investigations of Energy Materials with Soft and Hard X-Ray Spectroscopy. ECS Meeting Abstracts, 2018, , .	0.0	Ο